JOURNAL OF MAGNETIC RESONANCE **125,** 1–7 (1997)
ARTICLE NO. MN961071

^{17}O-Decoupled Proton MR Spectroscopy and Imaging in a Tissue Model

ALAN H. STOLPEN,* RAVINDER REDDY, AND JOHN S. LEIGH

Metabolic Magnetic Resonance Research and Computing Center, Department of Radiology, Hospital of the University of Pennsylvania, 3400 Spruce Street, Philadelphia, Pennsylvania 19104

Received May 28, 1996; revised October 22, 1996

^{17}O-decoupled proton MR spectroscopy and imaging were implemented at 2 T. Their sensitivity and accuracy *in vitro* were examined using semisolid tissue phantoms doped with $H_2{}^{17}O$. A double-tuned solenoidal coil was used to irradiate the same volume of ^{17}O and ^{1}H nuclei, as well as to facilitate direct calibration of the decoupling power. Decoupling efficiency was optimized as was ^{17}O detection sensitivity. Decoupling was most efficient at RF amplitudes below 2.5 kHz (expressed as $\gamma[^{17}O] \times H_1$), which is within the limits of the acceptable specific absorption rate. Propagation of error analysis demonstrated that ^{17}O detection sensitivity is optimal at a TE equal to the T_2 of ^{17}O-depleted water protons. Based on Meiboom's work, a simple theory was formulated for estimating the transverse relaxivity of $H_2{}^{17}O$ and the proton signal enhancement produced by decoupling. There was excellent agreement between theory and experiment. Overall, ^{17}O-decoupled spectroscopy and imaging were highly sensitive and accurate in quantifying $H_2{}^{17}O$ *in vitro*.

INTRODUCTION

^{17}O is a safe, nonradioactive oxygen isotope of nuclear spin-$\frac{5}{2}$ (*1*). $H_2{}^{17}O$ produces an ^{17}O NMR signal, whereas $^{17}O_2$ does not (*2*). Biophysicists have used direct ^{17}O NMR to measure the rate at which exogenous $^{17}O_2$ is converted to $H_2{}^{17}O$ by oxidative phosphorylation (*3–8*). ^{17}O NMR has also been used to measure tissue perfusion, capillary permeability, and water homeostasis (*4, 5, 8, 9*). However, the sensitivity of direct ^{17}O NMR is poor because ^{17}O nuclei have a small gyromagnetic ratio ($\gamma[^1H]/\gamma[^{17}O] \approx 8$), a short T_2 relaxation time (<6 ms), and a low natural abundance (0.037 at.%) (*10, 11*). Moreover, ^{17}O quantitation by direct methods is inaccurate due to quadrupolar interactions and multiple-quantum coherences. More than 30 years ago, Meiboom and co-workers showed that spin–spin coupling (i.e., *J* coupling) between ^{17}O and ^{1}H nuclei reduces proton $T_{1\rho}$ relaxation times (*12–16*). Their observations provided a strategy for detecting ^{17}O indirectly—and with greater sensitivity—by proton NMR.

T_2-weighted proton NMR methods have been used to quantify relative $H_2{}^{17}O$ concentrations in tissues *in vivo* (*3, 17–21*). In these methods, errors in the calculated $H_2{}^{17}O$ concentration can arise from spatial misregistration and ^{17}O-independent changes in tissue T_2. Ronen and Navon have introduced a novel method for realizing the full potential of indirect ^{17}O detection by T_2-weighted proton NMR (*22*). Their method uses radiofrequency irradiation at the ^{17}O resonance frequency, applied during evolution of the proton spin echo, to decouple [^{17}O–^{1}H] spin–spin coupling and thereby prolong proton T_2 relaxation times. Ronen and Navon have shown that ^{17}O-decoupled NMR can be used to detect $H_2{}^{17}O$ in aqueous phantoms at 8.4 T. To our knowledge, the decoupling method has not been critically evaluated with respect to accuracy in quantifying $H_2{}^{17}O$, optimization of experimental parameters, or sensitivity for $H_2{}^{17}O$ detection. In this article we formulate a theory of ^{17}O relaxivity and describe the implementation of ^{17}O-decoupled MR spectroscopy and imaging of semisolid tissue phantoms at a clinically relevant magnetic field strength.

THEORY

$H_2{}^{17}O$ was modeled as a T_2-type MR contrast agent. The standard mathematical formalism for these agents at low concentrations is

$$\frac{1}{T_2} = \frac{1}{T_2^0} + R_2 f, \qquad [1]$$

where T_2^0 is the proton T_2 of ^{17}O-depleted tissue, f is the concentration of $H_2{}^{17}O$, and R_2 is the transverse relaxivity in units of $(\text{at.}\%)^{-1}\ \text{s}^{-1}$. We now derive an expression for R_2 starting with Meiboom's equation for $H_2{}^{17}O$-dependent changes in proton $T_{1\rho}$ (Eq. [2] of Ref. *13*). This equation assumes that one of the following conditions obtains: (1) proton exchange is rapid, or (2) the proton spectrum is dominated by a central line (i.e., the ^{17}O atom fraction is very low). Assuming a symmetric distribution of the ^{17}O multi-

* To whom correspondence should be addressed.

1090-7807/97 $25.00

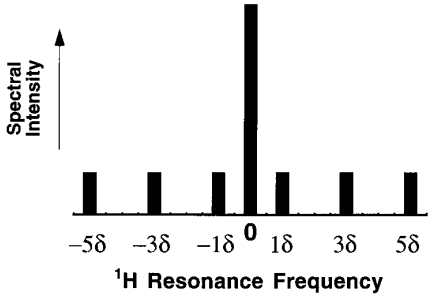

FIG. 1. Idealized ^{1}H spectrum of ^{17}O-enriched water. Protons bound to ^{16}O produce the dominant central peak at zero offset, whereas protons bound to ^{17}O are split into a sextet—one peak for each ^{17}O nuclear spin state. In deriving Eq. [2], these peaks are assumed to be of equal height, symmetrically distributed about the dominant central peak, and separated by $J = 2\delta = 91$ Hz.

plet about the dominant central line and equal population of the ^{17}O spin states (see Fig. 1), evaluation of Meiboom's Eq. [2] for $\omega_1 = 0$ yields

$$R_2 = \frac{\tau\delta^2}{3}\left(\frac{1}{1+\tau^2\delta^2} + \frac{9}{1+9\tau^2\delta^2} + \frac{25}{1+25\tau^2\delta^2}\right), \quad [2]$$

where τ is the proton exchange time and $\delta = J/2$. Burnett and Zeltmann have measured an [^{17}O–^{1}H] J-coupling constant of 91 Hz under fast exchange conditions (*23*). Figure 2 shows the variation of R_2 in Eq. [2] as a function of τ, evaluated for $J = 91$ Hz. R_2 reaches a theoretical maximum value of 3.9 (at.%)$^{-1}$ s^{-1} at $\tau = 0.9$ ms. Meiboom previously reported a τ of 1.1 ms (at 60 MHz) in ^{17}O-enriched water at neutral pH (*13*).

Proton signal intensity in the absence (S_0) and presence (S_{DC}) of ^{17}O decoupling can be expressed by the equations

$$S_0 = S\exp\left[-\mathrm{TE}\times\left(\frac{1}{T_2^0} + R_2 f\right)\right] \quad [3]$$

and

$$S_{DC} = S\exp\left[-\mathrm{TE}\times\left(\frac{1}{T_2^0} + R_2 f\times\{1-d\}\right)\right], \quad [4]$$

where d is the efficiency of ^{17}O decoupling and S is the proton signal intensity for TR $\gg T_1$ and TE $\ll T_2$. Highly efficient ^{17}O decoupling effectively sets R_2 equal to zero. The fractional change in proton signal intensity produced by ^{17}O decoupling (denoted $\Delta S/S_0$, where $\Delta S = S_{DC} - S_0$) is derived from Eqs. [3] and [4],

$$\frac{\Delta S}{S_0} = \exp(\mathrm{TE}\ R_2 fd) - 1 \quad [5]$$

which in the limit (TE $R_2 fd$) $\ll 1$ can be approximated by $\Delta S/S_0 \approx$ TE $R_2 fd$. The ^{17}O atom fraction is determined directly from S_{DC} and S_0 in Eqs. [3] and [4] as follows:

$$f = \frac{\ln(S_{DC}/S_0)}{\mathrm{TE}\ R_2 d}. \quad [6]$$

Equations [5] and [6] were used to extract the absolute $H_2{}^{17}O$ concentration from ^{17}O-decoupled proton MR spectroscopy and imaging data.

Propagation of error analysis was used to show how noise in the MR measurement of S_0 and S_{DC} (both denoted σ_S) is propagated to an error in the determination of $H_2{}^{17}O$ concentration (denoted σ_f):

$$\sigma_f^2 = \left(\frac{\partial f}{\partial S_0}\right)^2\sigma_S^2 + \left(\frac{\partial f}{\partial S_{DC}}\right)^2\sigma_S^2. \quad [7]$$

Equation [7] assumes that noise associated with the measurement of S_0 and S_{DC} is the same and is uncorrelated (i.e., the covariance is zero) (*24*). After substituting Eq. [6] into Eq. [7], taking partial derivatives, and normalizing σ_f with respect to f, we obtain

$$\frac{\sigma_f}{f} = \frac{\sigma_S(1/S_{DC}^2 + 1/S_0^2)^{1/2}}{\ln(S_{DC}/S_0)}. \quad [8]$$

The quantity σ_f/f is the normalized error in f. Substituting

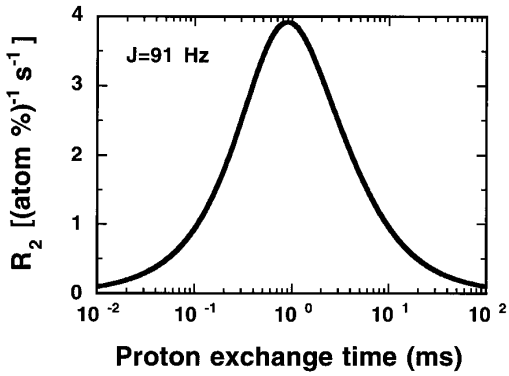

FIG. 2. Theoretical plot showing variation of R_2 with proton chemical exchange time (τ). Equation [2] was evaluated for $\tau = 0.01$–100 ms and $\delta = 91/4\pi$ rad/s. The maximum value of $R_2 = 3.9$ (at.%)$^{-1}$ s^{-1} occurs at $\tau = 0.9$ ms.

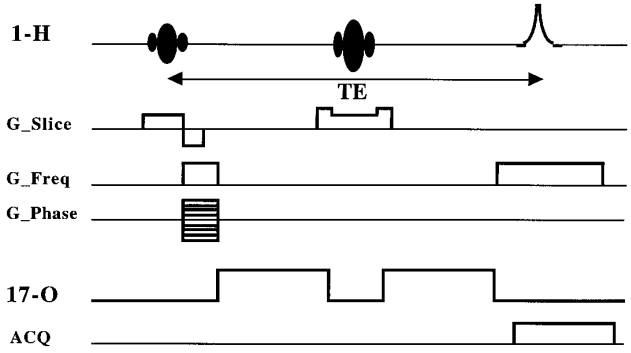

FIG. 3. Pulse sequence for ^{17}O-decoupled proton MR spectroscopy and imaging. Both sequences are based on a conventional 90°—τ—180°—τ—acquire spin-echo pulse sequence. A rectangular, low-power ^{17}O decoupling RF pulse is applied between the 90° and 180° RF pulses and then again between the 180° pulse and signal acquisition. For two-dimensional MR imaging, the hard RF pulses used in spectroscopy are replaced with truncated sinc pulses and the *X*, *Y*, and *Z* gradients are played out in the usual manner.

Eqs. [3] and [4] into Eq. [8] yields an explicit expression for σ_f/f as a function of TE,

$$\frac{\sigma_f}{f} = \left(\frac{\sigma_S}{S}\right) \times \frac{\{1 + \exp(-2Td\beta)\}^{1/2}}{Td\beta \exp\{-T(1+\beta)\}}, \qquad [9]$$

where we have introduced the substitutions

$$T \equiv \mathrm{TE}/T_2^0 \quad \text{and} \quad \beta \equiv R_2 T_2^0 f.$$

The term σ_S/S in Eq. [9] represents the reciprocal of the signal-to-noise ratio (SNR) for the proton NMR measurement.

MATERIALS AND METHODS

^{17}O-enriched water (25.7 at.%) was obtained from Isotech (Miamisburg, Ohio); porcine skin gelatin and sodium azide were obtained from Sigma (St. Louis, Missouri). Two hundred microliter, semisolid tissue phantoms containing 5% gelatin were prepared in 6 × 50 mm borosilicate glass tubes and doped with ^{17}O-enriched water to yield final ^{17}O concentrations between 0.037 (natural abundance) and 2 at.%. The pH was adjusted to 7.4 using sodium hydroxide. One millimolar sodium azide was added to prevent bacterial growth.

All experiments were performed on a 2 T superconducting magnet interfaced to a custom-built NMR spectrometer equipped with a broadband transmitter. An eight-turn solenoidal RF coil was custom-built and double-tuned to the ^{17}O (11.7 MHz) and ^{1}H (86.3 MHz) resonance frequencies, according to the method of Schnall *et al.* (*25*). T_1 and T_2 relaxation times were measured using 20-point spectroscopic inversion recovery and conventional spin-echo sequences, respectively. The ^{17}O-decoupled proton NMR pulse sequence is shown in Fig. 3. ^{17}O decoupling was performed during evolution of the proton spin echo by applying a single, low-power, rectangular RF pulse at the ^{17}O resonance frequency. ^{17}O decoupling amplitude was expressed as the product $\gamma[^{17}\mathrm{O}] \times H_1$ (in units of kilohertz), where H_1 is the RF magnetic field. The amplitude of the ^{17}O decoupling pulse was calibrated directly from the ^{17}O 90° pulsewidth (denoted $\tau_{90°}$) and RF attenuation; $\tau_{90°}$ was typically 16–22 μs and RF amplitude was typically 0–30% of maximum.

For spectroscopy experiments, half-echoes containing 2048 data points were acquired at 5 kHz bandwidth and processed with 3 Hz of exponential weighting. Peak heights of the magnitude spectra were determined in the absence and presence of ^{17}O decoupling. TR was 12 s ($\approx 5T_1$) and TE was 20–700 ms.

Proton MR imaging was performed using a conventional spin-echo pulse sequence modified for ^{17}O decoupling (see Fig. 3). A cluster of three phantoms was placed in a custom-built local gradient set which delivered a maximum gradient strength of 8 G/cm along the readout axis. The imaging parameters were as follows: 1 mm slice thickness, 2 × 2 cm field-of-view, 256 × 128 matrix, 20 kHz bandwidth, TR = 5 s, TE = 200 ms, and one signal average. Interleaved, ^{17}O-decoupled (3 kHz amplitude), and nondecoupled, asymmetric echoes were acquired and processed with 3 Hz of exponential weighting. Region-of-interest (ROI) measurements were obtained for each phantom from a post-processed image representing the natural logarithm of the ratio of images obtained with and without ^{17}O decoupling (''log-ratio'' image). ROI values from the log-ratio image were plotted as a histogram; the dominant peak in the histogram was selected, and the mean value was obtained from the Gaussian best fitting the selected peak.

RESULTS

There was a linear relationship between $H_2{}^{17}O$ concentration and proton T_2 relaxation rate (correlation coefficient = 0.998) for the isotope-enriched semisolid gelatin phantoms (Fig. 4). R_2 and T_2^0 were calculated from the slope and *y* intercept, respectively, of the line best fitting the plot of $1/T_2$ versus $H_2{}^{17}O$ concentration. The best-fit values of R_2 and T_2^0 were 3.3 $(\mathrm{at.\%})^{-1}\ \mathrm{s}^{-1}$ and 550 ms, respectively. $H_2{}^{17}O$ had little effect on T_1 relaxivity: T_1 was approximately 2.5 s at all $H_2{}^{17}O$ concentrations, and R_1 was less than 0.01 $(\mathrm{at.\%})^{-1}\ \mathrm{s}^{-1}$.

The effect of ^{17}O decoupling amplitude on decoupling efficiency was investigated using proton MR spectroscopy. The fractional change in proton signal intensity (i.e., $\Delta S/S_0$), which was assumed to be a measure of ^{17}O decoupling efficiency, was examined for ^{17}O decoupling amplitudes of 0–3.4 kHz, TR = 12 s, and TE = 600 ms. $\Delta S/S_0$ reached a stable plateau for all $H_2{}^{17}O$ concentrations studied (Fig. 5A). At the highest $H_2{}^{17}O$ concentration examined (2 at.%), $\Delta S/S_0$ reached a plateau at 2.3 kHz decoupling amplitude,

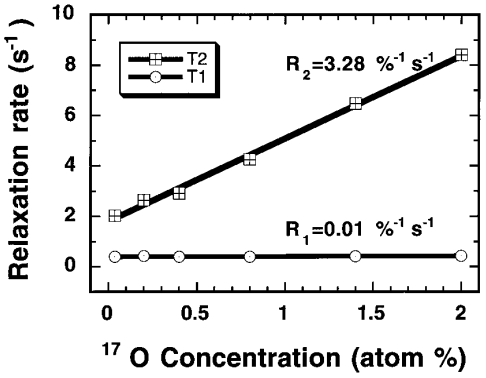

FIG. 4. Proton relaxivity plots of $H_2{}^{17}O$ in semisolid gelatin phantoms at 2 T. For concentrations between 0.037 and 2 at.%, $H_2{}^{17}O$ produced a linear increase in the transverse relaxation rate ($1/T_2$, upper line), but virtually no increase in the longitudinal relaxation rate ($1/T_1$, lower line). R_1 and R_2 for $H_2{}^{17}O$ were calculated from the slope of the line best fitting the corresponding relaxivity plot.

whereas at the lowest $H_2{}^{17}O$ concentration (0.037 at.%—natural abundance), the plateau was reached at 0.7 kHz. Overall, we found that higher decoupling amplitudes were required to reach the plateau in phantoms containing higher $H_2{}^{17}O$ concentrations. In subsequent experiments we used decoupling amplitudes of 2–3 kHz. For the phantom containing only natural abundance $H_2{}^{17}O$ (0.037 at.%), the percentage increase in proton signal intensity reached a maximum value of 12.4% at a decoupling amplitude of 1.7 kHz (Fig. 5B).

The effect of TE on proton signal intensity was investigated using ^{17}O-decoupled MR spectroscopy. The fractional and absolute changes in proton signal intensity ($\Delta S/S_0$ and ΔS, respectively) were examined in the ^{17}O-enriched semisolid gelatin phantoms at a decoupling amplitude of 2.4 kHz, TR = 12 s, and TE between 20 and 700 ms. Figures 6A and 6B show plots of $\Delta S/S_0$ and ΔS versus TE, respectively. As predicted by the solution to $d(\Delta S)/d(\mathrm{TE}) = 0$, ΔS reached a maximum value at $\mathrm{TE} \approx \ln(1 + R_2 T_2^0 f)/(R_2 f)$. In contrast, $\Delta S/S_0$ was an increasing function of TE over the range 20–700 ms, as predicted by Eq. [5]. This latter result leads to the absurd conclusion that an infinitely long TE should be used to obtain optimal signal enhancement.

To resolve this dilemma regarding the correct strategy for optimizing TE and maximizing the sensitivity of the decoupling method for $H_2{}^{17}O$ detection, we used propagation of error analysis. Using Eq. [9], we determined the TE (denoted $\mathrm{TE_{OPT}}$) that minimized σ_f/f for values of β between 0.001 and 10 and ^{17}O decoupling efficiencies of 10 and 100%. Values of β varied from 0.07 to 3.63 (dimensionless) in the $H_2{}^{17}O$-enriched semisolid gelatin phantoms. Figure 7 shows plots of $\mathrm{TE_{OPT}}/T_2^0$ versus β. We found that $\mathrm{TE_{OPT}} \approx T_2^0$ for the range of β values most likely to be encountered *in vivo* (i.e., $\beta < 0.1$), whereas $\mathrm{TE_{OPT}} < T_2^0$ for $\beta > 0.1$.

The accuracy of the $H_2{}^{17}O$ quantitation by ^{17}O-decoupled proton MR spectroscopy was assessed in isotope-enriched semisolid gelatin phantoms at 2.3 kHz decoupling amplitude. Theoretically predicted values of $\Delta S/S_0$ were calculated from Eq. [5] for TE = 600 ms, d = 100%, R_2 = 3.3 (at.%)$^{-1}$ s^{-1}, and the appropriate $H_2{}^{17}O$ concentration. Agreement between theory and experiment was excellent at all $H_2{}^{17}O$ concentrations except the highest concentration (2 at.%), where theory overestimated the concentration by 20% (Fig. 8).

^{17}O-decoupled proton MR imaging was used to quantify $H_2{}^{17}O$ concentrations in three isotope-enriched semisolid gelatin phantoms. To reduce magnetic susceptibility artifacts in the phantom assembly, the TE was reduced from 550 ms (as recommended by propagation of error analysis; see Fig.

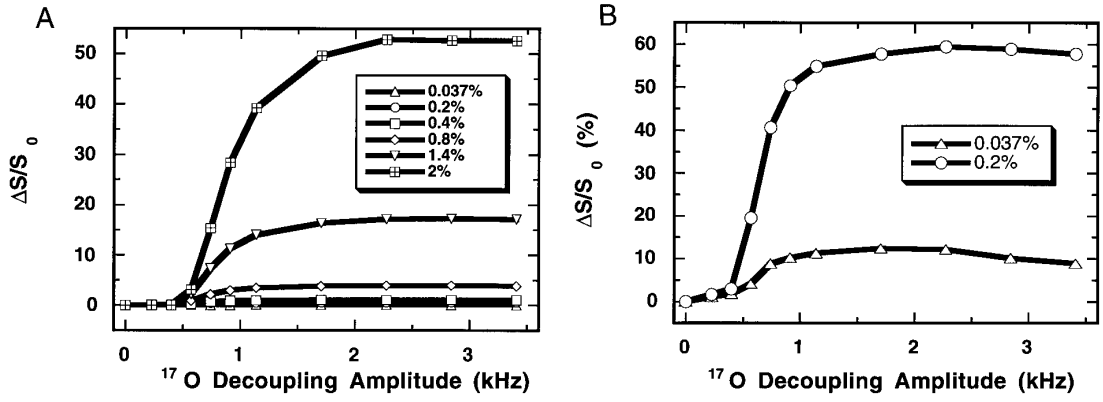

FIG. 5. Decoupling efficiency as a function of ^{17}O decoupling amplitude. (A) Fractional increase in proton MR spectroscopic signal intensity produced by ^{17}O decoupling ($\Delta S/S_0$) was determined for each of six phantoms containing different concentrations of $H_2{}^{17}O$ (see inset for symbol legend) and decoupling amplitudes of 0–3.4 kHz. (B) Data from A for phantoms containing 0.037 and 0.2 at.% $H_2{}^{17}O$ were replotted for better visualization. ^{17}O decoupling increased proton signal intensity by 12.4% in the phantom containing natural abundance ^{17}O (lower curve in B).

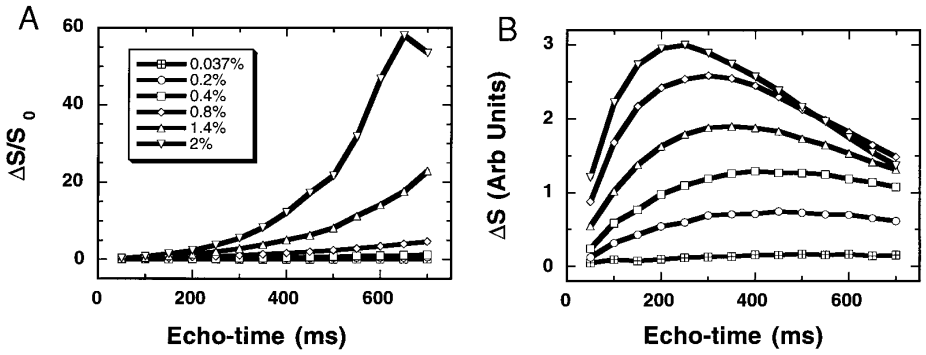

FIG. 6. ^{17}O decoupling efficiency as a function of TE. Fractional increase (A) and absolute increase (B) in proton MR spectroscopic signal intensity for phantoms containing six different concentrations of $H_2{}^{17}O$ (see inset for symbol legend) were determined at 50–700 ms TE and 2.4 kHz decoupling amplitude. Plots of ΔS versus TE (B) revealed discrete maxima at TE $\approx \ln(1 + R_2T_2^0f)/(R_2f)$, whereas $\Delta S/S_0$ (A) was an increasing function of TE without discrete maxima.

7) to 200 ms. The optimal TE ($\approx T_2^0$) for most tissues *in vivo* is expected to be less than 150 ms. Figure 9 shows the log ratio of T_2-weighted spin-echo images obtained in the presence and absence of 3 kHz ^{17}O decoupling. According to Eq. [6], pixel intensity should be proportional to $H_2{}^{17}O$ concentration. Mean pixel values for each phantom in the log-ratio image were determined by ROI analysis. These values were substituted into Eq. [6] and used to calculate the absolute $H_2{}^{17}O$ concentration for each phantom, assuming TE = 200 ms, d = 100%, and R_2 = 3.3 (at.%)$^{-1}$ s^{-1}. Table 1 shows a comparison of actual $H_2{}^{17}O$ concentrations and those calculated using the ^{17}O-decoupled proton MR imaging method. There was good correlation between the actual and calculated values.

DISCUSSION

Our data show that the efficiency of ^{17}O decoupling varied with decoupling amplitude and $H_2{}^{17}O$ concentration: higher amplitudes were required to maximally decouple higher concentrations. These results differ from those of Ronen and Navon, who showed that decoupling efficiency was independent of $H_2{}^{17}O$ concentration between 0.27 and 4.64 at.% (*22*). Overall, we found that decoupling amplitudes between 0.7 and 2.3 kHz produced the most efficient decoupling. These RF amplitudes satisfy the theoretical requirement for efficient decoupling, mainly $\gamma[^{17}O] \times H_1 \gg J$, where J = 91 Hz. Moreover, these RF amplitudes are likely safe for patients inasmuch as they fall within allowable limits for the specific absorption rate at 1.5 T (*26, 27*). Our data do not prove that ^{17}O decoupling was 100% efficient. In fact, a systematic underestimation of the true $H_2{}^{17}O$ concentration would result from erroneously assuming a decoupling efficiency of 100%.

Our efforts to optimize TE initially led to contradictory results. Propagation of error analysis provided a cogent strat-

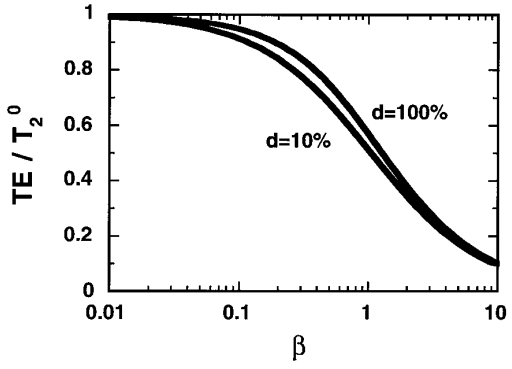

FIG. 7. Optimization of TE by propagation of error analysis. Equation [9] describes the relative uncertainty in the $H_2{}^{17}O$ concentration (denoted σ_f/f) as determined by ^{17}O-decoupled proton MR. The TE minimizing σ_f/f was determined numerically for values of the parameter β ($\equiv R_2T_2^0f$) between 0.001 and 10 and decoupling efficiencies of 10 and 100%. The analysis shows that for $\beta < 0.1$ (the condition most likely to obtain *in vivo*), the optimal TE is approximately T_2^0.

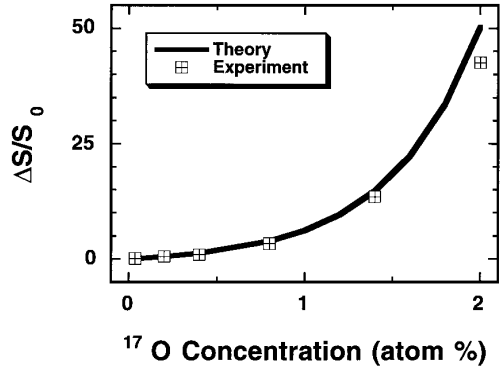

FIG. 8. Comparison of theoretical and experimental determinations of $H_2{}^{17}O$ concentration by ^{17}O-decoupled proton MR spectroscopy. Experimental data were acquired with 2.4 kHz decoupling amplitude and 600 ms echo time. Theoretical data points were obtained from Eq. [5] for ^{17}O atomic fractions between 0.037 and 2.0, assuming an R_2 of 3.3 (at.%)$^{-1}$ s^{-1} and 100% decoupling efficiency. There is excellent agreement between the theoretical and experimental results, except at the highest $H_2{}^{17}O$ concentrations.

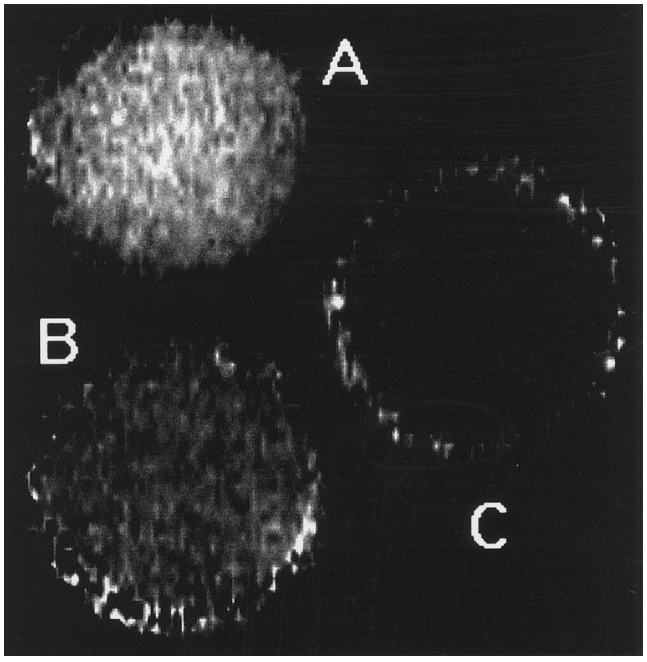

FIG. 9. ^{17}O-decoupled proton MR imaging. Phantoms containing ^{17}O atomic fractions of 0.4 (vial A), 0.2 (vial B), and 0.037 (vial C) were immersed in a water-filled glass tube and imaged with and without 3 kHz decoupling (TR = 5 s, TE = 200 ms). The image depicts the natural logarithm of the ratio image (^{17}O-decoupled/nondecoupled). According to Eq. [6], pixel intensity should be proportional to $H_2{}^{17}O$ concentration. The vial containing 0.4 at.% ^{17}O (A) shows the highest signal intensity, whereas the vial containing natural abundance ^{17}O (C) shows the lowest intensity.

egy for optimizing TE and maximizing the $H_2{}^{17}O$ detection sensitivity of the decoupling method. Under conditions likely to obtain *in vivo,* error analysis showed that the optimal TE was approximately equal to the T_2^0 of the tissue under investigation. Ronen and Navon obtained a similar result using a different analytical method (*22*).

RF coils double-tuned to the ^{17}O and ^{1}H resonance frequencies have been used previously, but mainly to obtain proton localization images or to shim the main magnetic field in ^{17}O NMR studies (*3, 5, 7*). To our knowledge, ^{17}O-decoupled proton NMR has not previously been implemented with a double-tuned coil (*28*). Double-tuned coils offer the advantage of decoupling and exciting the same (or very similar) sample volumes and of reducing the hardware required to implement the ^{17}O decoupling method. Additionally, double-tuned coils permit direct calibration of the ^{17}O decoupling pulse. Ronen and Navon, who used separate ^{1}H and ^{17}O RF coils in their implementation of the decoupling method, were unable to directly measure the absolute RF amplitude of the ^{17}O decoupling pulse.

The ^{17}O detection sensitivity of the decoupling method depends on the R_2 of $H_2{}^{17}O$. We and others have previously reported R_2 values of 2.3 to 3.3 $(\text{at.}\%)^{-1}\ \text{s}^{-1}$ for $H_2{}^{17}O$ in a variety of aqueous media and at magnetic field strengths between 0.6 and 8.4 T (*22, 29–31*). We have determined that the theoretical maximum value for R_2 is 3.9 $(\text{at.}\%)^{-1}\ \text{s}^{-1}$. Meiboom showed that R_2 is strongly dependent on pH, achieving a maximum value near neutrality, and furthermore, that pH buffers can decrease R_2 by increasing the proton exchange rate (*12–14, 16, 29, 32*). The neutral pH of most biological tissues ensures that R_2 will reside near its maximum value, although the plethora of pH buffers in tissue may reduce R_2. Our semisolid tissue phantoms had an R_2 of 3.3 $(\text{at.}\%)^{-1}\ \text{s}^{-1}$, which corresponds to a proton exchange time of 0.5 ms (Fig. 2); R_2 at the theoretical maximum corresponds to an exchange time of 0.9 ms. The shorter exchange time of the phantoms may be due to pH buffers or impurities.

Reddy and co-workers have described an indirect method, based on proton $T_{1\rho}$ dispersion imaging, for measuring $H_2{}^{17}O$ (*30*). Briefly, a pair of $T_{1\rho}$-weighted images are acquired at low ($<$0.5 kHz) and high ($>$1.2 kHz) spin-locking frequencies; the pixel intensity of the log-ratio image is proportional to the $H_2{}^{17}O$ concentration. Despite their apparent differences, the $T_{1\rho}$ dispersion and ^{17}O decoupling methods are similar in many respects. The ^{17}O decoupling pulse is analogous to the proton spin-locking pulse; $T_{1\rho}$-weighted images acquired at high and low spin-locking frequency are analogous to ^{17}O-decoupled and nondecoupled images, respectively; and the sensitivity for $H_2{}^{17}O$ detection by the decoupling method is proportional to TE $R_2 d$, whereas the sensitivity of the $T_{1\rho}$ dispersion method is proportional to the product of the spin-locking duration and $R_{1\rho}$ dispersion. Unlike the decoupling method, the $T_{1\rho}$ dispersion method can be implemented without special hardware, such as a double-tuned coil or broadband transmitter.

^{17}O-decoupled proton MR spectroscopy and imaging show great promise for accurate, highly sensitive, and noninvasive quantitation of regional oxidative metabolism and tissue perfusion. Strategies for improving the speed and sensitivity of the decoupling method, including the use of localized proton spectroscopy, are currently being explored. The high cost of ^{17}O-enriched chemicals remains one of the major drawbacks of the ^{17}O-based methods. We and others have demonstrated

TABLE 1
Accuracy of $H_2{}^{17}O$ Quantitation by ^{17}O-Decoupled Proton MR Imaging at 2 T

	^{17}O concentration (at. %)		
Vial:	A	B	C
Actual	0.4%	0.2%	0.037%
Measured[a]	0.42%	0.23%	0.024%

[a] $H_2{}^{17}O$ concentrations in the phantoms were calculated from Eq. [6] using ROI measurements from the log-ratio image depicted in Fig. 9, and assuming $R_2 = 3.3\ (\text{at.}\%)^{-1}\ \text{s}^{-1}$ and $d = 100\%$.

the applicability of the ^{17}O-decoupling method for quantifying ultralow $H_2{}^{17}O$ concentrations *in vitro* and for detecting exogenously administered $H_2{}^{17}O$ *in vivo* (*33–36*). We are currently using ^{17}O-decoupled proton MR to quantify cerebral oxygen consumption *in vivo.*

ACKNOWLEDGMENTS

The authors gratefully acknowledge technical assistance and careful review of the manuscript by Dr. Elizabeth Noyszewski and Sridhar Charagundla and helpful discussions with Dr. Alan C. McLaughlin. Dr. Stolpen is a scholar of the American Roentgen Ray Society. This work was supported by the NIH under Grants RR02305 and HL09049.

REFERENCES

1. D. Samuel, D. Wolf, A. Meshorer, and I. Wasserman, *in* ''Proceedings of the First International Conference on Stable Isotopes in Chemistry, Biology, and Medicine'' (P. D. Klein and S. V. Peterson, Eds.), p. 203, U.S. Atomic Energy Commission, Oak Ridge, Tennessee, 1973.
2. C. S. Irving and A. Lapidot, *Nature* **230,** 224 (1971).
3. T. Arai, S-i. Nakao, K. Mori, K. Ishimori, I. Morishima, T. Miyazawa, and B. Fritz-Zieroth, *Biochem. Biophys. Res. Commun.* **169,** 153 (1990).
4. T. Arai, K. Mori, S-i. Nakao, K. Watanabe, K. Kito, M. Aoki, H. Mori, S. Morikawa, and T. Inubushi, *Biochem. Biophys. Res. Commun.* **179,** 954 (1991).
5. J. Pekar, L. Ligeti, Z. Ruttner, R. C. Lyon, T. M. Sinwell, P. van Gelderen, D. Fiat, C. T. W. Moonen, and A. C. McLaughlin, *Magn. Reson. Med.* **21,** 313 (1991).
6. G. D. Mateescu, J. C. LaManna, D. W. Lust, L. M. Mars, and J. Tseng, Abstracts of the Society of Magnetic Resonance in Medicine, 10th Annual Meeting, San Francisco, p. 1031, 1991.
7. D. Fiat, L. Ligeti, R. C. Lyon, Z. Ruttner, J. Pekar, C. T. W. Moonen, and A. C. McLaughlin, *Magn. Reson. Med.* **24,** 370 (1992).
8. J. Pekar, T. Sinwell, L. Ligeti, A. S. Chesnick, J. A. Frank, and A. C. McLaughlin, *J. Cereb. Blood Flow Metabol.* **15,** 312 (1995).
9. G. D. Mateescu, G. M. Yvars, J. C. LaManna, D. W. Lust, and D. Sudilovsky, Abstracts of the Society of Magnetic Resonance in Medicine, 9th Annual Meeting, New York, p. 1236, 1990.
10. J. A. Glasel, *Proc. Natl. Acad. Sci. USA* **55,** 479 (1966).
11. B. B. Garrett, A. B. Denison, and S. W. Rabideau, *J. Phys. Chem.* **71,** 2606 (1967).
12. S. Meiboom, Z. Luz, and D. Gill, *J. Chem. Phys.* **27,** 1411 (1957).
13. S. Meiboom, *J. Chem. Phys.* **34,** 375 (1961).
14. Z. Luz and S. Meiboom, *J. Chem. Phys.* **39,** 366 (1963).
15. Z. Luz and S. Meiboom, *J. Am. Chem. Soc.* **85,** 3923 (1963).
16. Z. Luz and S. Meiboom, *J. Am. Chem. Soc.* **86,** 4764 (1964).
17. A. L. Hopkins and R. G. Barr, *Magn. Reson. Med.* **4,** 399 (1987).
18. A. L. Hopkins, E. M. Haacke, J. Tkach, R. G. Barr, and C. B. Bratton, *Magn. Reson. Med.* **7,** 222 (1988).
19. T. Arai, P. M. Gupte, S. E. Lasker, L. R. M. del Guercio, and K. Mori, *Crit. Care Med.* **17,** 1333 (1989).
20. K. K. Kwong, A. L. Hopkins, J. W. Belliveau, D. A. Chesler, L. M. Porkka, R. C. McKinstry, D. A. Finelli, G. J. Hunter, J. B. Moore, R. G. Barr, and B. R. Rosen, *Magn. Reson. Med.* **22,** 154 (1991).
21. A. L. Hopkins, W. D. Lust, E. M. Haacke, P. Wielopolski, R. G. Barr, and C. B. Bratton, *Magn. Reson. Med.* **22,** 167 (1991).
22. I. Ronen and G. Navon, *Magn. Reson. Med.* **32,** 789 (1994).
23. L. J. Burnett and A. H. Zeltmann, *J. Chem. Phys.* **60,** 4636 (1974).
24. P. R. Bevington, ''Data Reduction and Error Analysis in the Physical Sciences,'' McGraw–Hill, New York, 1969.
25. M. D. Schnall, V. H. Subramanian, J. S. Leigh, and B. Chance, *J. Magn. Reson.* **65,** 122 (1985).
26. P. A. Bottomley and W. A. Edelstein, *Med. Phys.* **8,** 510 (1981).
27. R. E. Sepponen, J. A. Pohjonen, J. T. Sipponen, and J. I. Tanttu, *J. Comput. Assist. Tomogr.* **9,** 1007 (1985).
28. R. Reddy, A. H. Stolpen, and J. S. Leigh, Abstracts of the Society of Magnetic Resonance, 3rd Annual Meeting, Nice, p. 1931, 1995.
29. H. N. Yeung and A. H. Lent, *Magn. Reson. Med.* **5,** 87 (1987).
30. R. Reddy, A. H. Stolpen, and J. S. Leigh, *J. Magn. Reson. B* **108,** 276 (1995).
31. A. H. Stolpen, R. Reddy, and J. S. Leigh, Abstracts of the Society of Magnetic Resonance, 3rd Annual Meeting, Nice, p. 527, 1995.
32. R. E. Glick and K. C. Tewari, *J. Chem. Phys.* **44,** 546 (1966).
33. S. R. Charagundla, R. Reddy, A. H. Stolpen, and J. S. Leigh, Abstracts of the International Society of Magnetic Resonance in Medicine, 4th Annual Meeting, New York, p. 377, 1996.
34. I. Ronen and G. Navon, Abstracts of the Society of Magnetic Resonance, 2nd Annual Meeting, San Francisco, p. 227, 1994.
35. G. Navon, J. H. Lee, H. Merkle, I. Ronen and K. Ugurbil, Abstracts of the 36th Experimental NMR Conference, Boston, p. 264, 1995.
36. R. R. Rizi, R. Reddy, A. H. Stolpen, S. R. Charagundla, and J. S. Leigh, Abstracts of the International Society of Magnetic Resonance in Medicine, 4th Annual Meeting, New York, p. 1364, 1996.